Advances in Computational Design, *Vol. 7, No. 1 (2022) 69-79*
DOI: https://doi.org/10.12989/acd.2022.7.1.069

An analytical approach for aeroelastic analysis of tail flutter

Amin Gharaei[1], Hamid Rabieyan-Najafabadi[2], Hossein Nejatbakhsh[3] and Ahmad Reza Ghasemi*[3]

[1]*Faculty of Engineering, Yazd University, Yazd, Iran*
[2]*Faculty of New Sciences and Technologies, University of Tehran, Tehran, Iran*
[3]*Faculty of Mechanical Engineering, University of Kashan, Kashan, Iran*

(Received September 2, 2021, Revised October 10, 2021, Accepted November 8, 2021)

Abstract. In this research, the aeroelastic instability of a tail section manufactured from aluminum isotropic material with different shell thickness investigated. For this purpose, the two degrees of freedom flutter analytical approach are used, which is accompanied with simulation by finite element analysis. Using finite element analysis, the geometry parameters such as the center of mass, the aerodynamic center and the shear center are determined. Also, by simulation of finite element method, the bending and torsional stiffnesses for various thickness of the airfoil section are determined. Furthermore, using Lagrange's methods the equations of motion are derived and modal frequency and critical torsional/bending modes are discussed. The results show that with increasing the thickness of the isotropic airfoil section, the flutter and divergence speeds increased. Compared of the obtained results with other research, indicates a good agreement and reliability of this method.

Keywords: aeroelastic instability; aluminum airfoil section; finite element analysis; flutter speed

1. Introduction

The flutter is a dangerous phenomenon encountered in flexible structures subjected to aerodynamic forces. This includes aircraft, buildings, telegraph wires, stop signs and bridges. The flutter occurs as results of mutual interaction of aerodynamic, structural and inertial forces, which can result in limitations in the operational condition or catastrophic failure of the aircraft. In an aircraft, as the speed of the wind increases, there may be a point at which the structural damping is insufficient to damp out the motions which are increasing due to aerodynamic energy being added to the structure. This vibration can cause structural failure and therefore considering flutter characteristics is an essential part of designing an aircraft.

The aerodynamic loads on the wings, tails, and blades often tolerate by the main spar structure that mostly manufactured of laminated composite materials. The aeroelasticity of a suspension bridge (Ding *et al*. 2002, Diana *et al*. 2004, Borri and Costa 2004) and nonlinear behavior in fluid-structure interaction of bridge decks (Grinderslev *et al*. 2018) have investigated. The flutter phenomena and aeroelastic stability of beam (Marzani and Viola 2003, Wang 2003) and plate

*Corresponding author, Professor, E-mail address: Ghasemi@Kashanu.ac.ir

http://www.techno-press.org/?journal=acd&subpage=7 ISSN: 2383-8477 (Print), 2466-0523 (Online)

(Mousavi and Yazdi 2019) have studied.

The dynamic stability of laminated composite plates using the ant colony optimization algorithm (Shafei and Shirzad 2017), the non-linear stability and elasto-plastic analysis of the composite structure (Cai *et al*. 2017), stability analysis of sandwich and functionally graded beams (Eltaher and Mohamed 2020), stability of cylinder (Taheri-Behrooz and Omidi 2018), shell (Lair *et al*. 2019) and plates (Mahmoud and Tounsi 2019) were studied presented in recent years.

An aerodynamic control method of the wind-induced instabilities of a long-span bridge was investigated by Omenzetter *et al*. (Omenzetter *et al*. 2000) They developed a mathematical model of aerodynamic passive control for suppression of wind-induced vibration in bridges and proposed critical wind speed and system's degree of stability to find the optimum configuration for control system (Omenzetter *et al*. 2000). Mastroddi *et al*. (Mastroddi *et al*. 2011, Dillinger *et al*. 2013) optimized the wing structures using the analytical model and finite element analysis for structural behaviors, flight dynamics and aeroelasticity operations. Also, the stiffness of the lower and upper shells of a composite wing were optimized by Dillinger *et al*. (Mastroddi *et al*. 2011, Dillinger *et al*. 2013). They used the in-plane and bending stiffness and laminate thicknesses as design variables, and mass, strength, buckling, aerodynamic twist, and aileron effectiveness are optimized. Stodieck *et al*. (Stodieck *et al*. 2017, Li *et al*. 2020) were used tow-steered composites in upper and lower wing skins with laminate thickness and rotation angle variables to model the aeroelastically tailored of wing-box.

The aeroelasticity behaviors of wind turbine blades have attracted researchers' attention. Li *et al*. (Li *et al*. 2020) investigated the aerodynamic and aeroelastic characterization of flexible wind turbine blades under periodic unsteady inflows as including the wind shear, tower shadow, and yawed inflow. The numerical and analytical investigation of composite wind turbine blades based on FAR and JAR standards using two degrees of freedom flutter carried out by Ghasemi *et al*. (Ghasemi *et al*. 2014, Ghasemi and Mohandes 2016). They have not examined the airfoil parameters as torsional and bending stiffness, and simulated 3-D composite blades using finite element methods. Evans *et al*. (Evans *et al*. 2018) were studied the aeroelastic behavior of a small horizontal-axis wind turbine and developed a model based on blade and tail fin aerodynamic effects, blade and tower structural response, and variable speed control but did not more attention to airfoil section of the blades and torsional-bending coupling of the rotor.

In this research with more attention to coupled bending-torsional vibrations, the aeroelasticity behavior and flutter speed of a V-tail aircraft are studied. The geometry parameters of airfoil section as: center of mass, the aerodynamic center and the shear center are determined using the ANSYS commercial software. Then using simulation the symmetric airfoil and apply aerodynamic loading for various skin thicknesses, the bending and torsional stiffnesses are determined. Finally, using Lagrange's methods the equations of motion are derived and modal frequency and critical torsional/bending modes are discussed. Furthermore, the results of this coupled model have been compared with the resulted that obtained from other formulation and verified.

2. Problem descriptions and governing equations

2.1 Geometrical parameters

In this research, the aeroelastic behavior and flutter analysis of a V-tail aircraft have investigated. The airfoil section of the tail is shown in Fig. 1 and geometrical parameters are

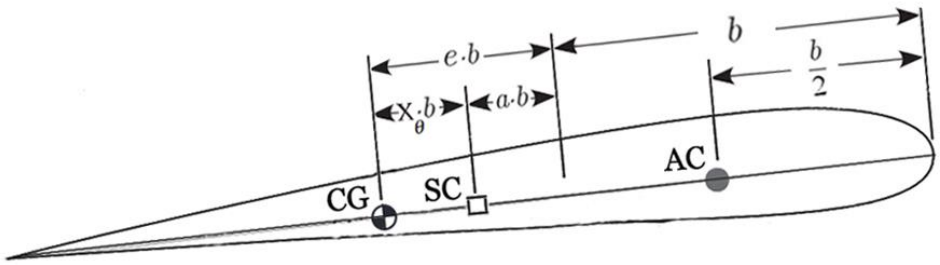

Fig. 1 Geometry of the tail typical section with aeroelastic points

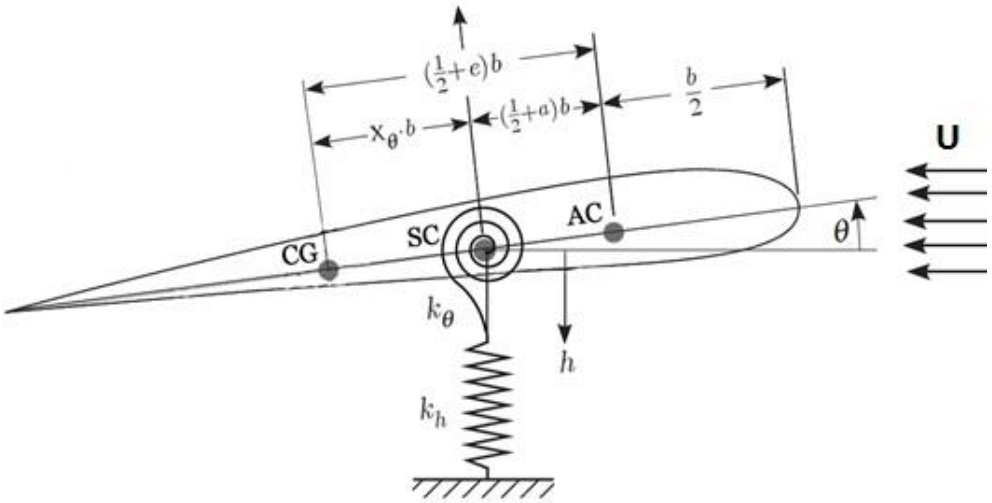

Fig. 2 Tail section with two degrees of freedom and bending/torsional spring stiffnesses

detected. The chord length is C and the half of chord determined as b in this figure. The points AC, SC and CG refer to the aerodynamic center, shear center or reference point in the flutter analysis and the center of gravity, respectively. The location of the point AC and CG are determined using dimensionless parameters e and a that shown in Fig. 1, which $x_\theta = e - a$. When these parameters are zero, the point lies on the mid chord, and when they are positive/negative, the points lie toward the trailing/leading edges.

The wing structural bending and torsional stiffnesses are modeled using discrete linear spring as shown in Fig. 2 (Ghasemi *et al*. 2014, Ghasemi and Mohandes 2016, Hodges and Pierce 2011). For V-tail that has a smooth taper in the aircraft, the length of chord in the mid-length of the tail is selected for analysis and the bending and torsional stiffnesses are determined based on material properties and thickness of the skin-airfoil.

2.2 Governing equations

For the flutter analysis, the equations of motion are derived using Lagrange's equations

(Hodges and Pierce 2011). For this object the center offset of mass denoted by Eq. (1) and the kinetic and potential energies are determined by Eqs. (2) and (3) as following:

$$x_\theta = e - a \qquad -1 \le e \le +1 \qquad -1 \le a \le +1 \tag{1}$$

$$P = \frac{1}{2}k_h h^2 + \frac{1}{2}k_\theta \theta^2 \tag{2}$$

$$K = \frac{1}{2}m v_c . v_c + \frac{1}{2}I_{CG}\dot{\theta}^2 \tag{3}$$

In the above equations k_h, k_θ, m and I_{CG} are bending stiffness, torsional stiffness, mass and moment of inertia about center of gravity, respectively. Also, h, θ, v_c and θ are linear displacement, rotational angle of two degrees of freedom and velocity of them, respectively.

Using simplicity in Lagrange's Eqs. (2) and (3), for the aerodynamics behavior of the airfoil section, the equation of motion can be re-written as follows:

$$m\left(\ddot{h} + bx_\theta \ddot{\theta}\right) + k_h h = -L \tag{4}$$

$$I_{sc}\ddot{\theta} + mbx_\theta \ddot{h} + k_\theta \theta = b\left(\frac{1}{2} + a\right)L \tag{5}$$

$$L = 2\pi\rho_\infty b U^2 \theta \tag{6}$$

where L, ρ_∞ and U denoted to the lift aerodynamic force, air density and air speed, respectively. Also, $I_{SC} = I_{CG} + mb^2x^2_\theta$ (Ghasemi *et al*. 2014, Hodges and Pierce 2011). By noting to the natural bending and torsional frequency in the zero speed, we have:

$$\omega_h = \sqrt{\frac{k_h}{m}} \qquad \omega_\theta = \sqrt{\frac{k_\theta}{I_{SC}}} \tag{7}$$

To simplify the problem, we consider the following four dimensionless variables as follows:

$$r^2 = \frac{I_{SC}}{mb^2} \qquad \sigma = \frac{\omega_h}{\omega_\theta} \qquad \mu = \frac{m}{\rho_\infty \pi b^2} \qquad V = \frac{U}{b\omega_\theta} \tag{8}$$

where r, σ, μ and V are the dimensionless radius of gyration of the airfoil section about the shear center SC, ratio of the uncoupled bending to torsional frequencies, the model mass to the mass of the air affected by the model, and reduced velocity as the dimensionless free stream speed of the air, respectively.

The response of the linear displacement (h) and rotational angle (θ) can be assumed as exponential form and with the substitutions $h = \bar{h}e^{vt}$ and $\theta = \bar{\theta}e^{vt}$ yielding:

$$\begin{bmatrix} s^2 + \sigma^2 & s^2 x_\theta + \frac{2V^2}{\mu} \\ s^2 x_\theta & s^2 r^2 + r^2 - \frac{2V^2}{\mu}\left(\frac{1}{2} + a\right) \end{bmatrix} \begin{bmatrix} \frac{\bar{h}}{b} \\ \bar{\theta} \end{bmatrix} = \begin{Bmatrix} 0 \\ 0 \end{Bmatrix} \tag{9}$$

To obtain a nontrivial solution, the determinant of the coefficient matrix must be set equal to zero. There are two complex conjugate pairs of roots, that $S_{1,2} = (\Gamma_{1,2} \pm i\Omega_{1,2}) / \omega_\theta$. For a given airfoil section, the behavior of the real and imaginary part of the complex roots as functions of V are calculated and discussed. The dynamic instability referred to as flutter, for which $\Gamma_k \geq 0$, $\Omega_k \neq 0$, and the unstable condition for $\Omega_k = 0$, and the divergence boundary occurs when $\Gamma_k = \Omega_k = 0$ (Hodges and Pierce 2011). The smallest value of V gives divergent oscillations, whose value is $V_F = U_F / b\omega_\theta$, where U_F is the flutter speed.

In the next section, this formulation has applied for a V-tail hollow airfoil section (a thin wall section without spar). The aeroelastic stability and flutter speed are investigated for different materials and various thicknesses, and for this real section has obtained and discussed.

3. Results and discussions

3.1 Geometrical parameters analysis

Various thicknesses and different materials as isotopic materials are investigated in this research and compared with thicknesses in real V-tail section. The thicknesses of the skin suggested as 0.5, 1, 1.5 and 2 mm in Table 1. The chord length of the airfoil is C = 431 mm, and the aerodynamic parameters are determined and presented in Table 1 using ANSYS commercial software. It should be noted that, a and $x_\theta = e - a$ are dimensionless parameters in this Table. Also, C.G, S.C, A and I_{SC} denoted to the center of gravity, shear center, area of airfoil and inertia about shear center, respectively.

To determine the bending/torsional stiffnesses using finite element method a new approach is employed. The value of the flexural wing section is the ratio of the force applied at the bending section to the value of deflection of that section relative to the root section. Also, the torsional stiffness of the wing is calculated as the ratio of the momentum to the angular rotation of the airfoil section. The torsional momentum produced by a pair of vertical forces applied to a frame fixed at the measuring section (Aleksandrowicz and Lucjanek 1958).

A two-dimensional reference section airfoil is shown in Fig. 3(a), that bending/torsional loading were applied to obtain bending/torsional stiffnesses of the thin airfoil section of the tail. For bending stiffness, the values of tail stiffness are the ratio of the force F_h applied at the bending section to the value of deflection relative to root (h) as shown in Fig. 3(b). The torsional stiffness is the ratio of the bending moment M_θ applied at the root section to the angle of rotation of the reference section relative to the root section (θ) as shown in Fig. 3(c) and mentioned in Eq. (10).

$$k_\theta = \frac{M_\theta}{\theta} \qquad k_h = \frac{F_h}{h} \tag{10}$$

Table 1 Geometric dimensions of hollow-airfoil section based on different thicknesses

Thickness: t (mm)	C.G (mm) from LE	S.C (mm) from LE	A (mm^2)	I_{SC} (m^4)	e	a
0.5	210.723	111.260	430.7	2.96E-02	-2.22E-02	-4.84E-01
1	208.093	116.398	849.1	5.40E-02	-3.44E-02	-4.60E-01
1.5	206.045	119.840	1258.7	7.57E-02	-4.39E-02	-4.44E-01
2	204.324	122.792	1661.0	9.51E-02	-5.19E-02	-4.30E-01

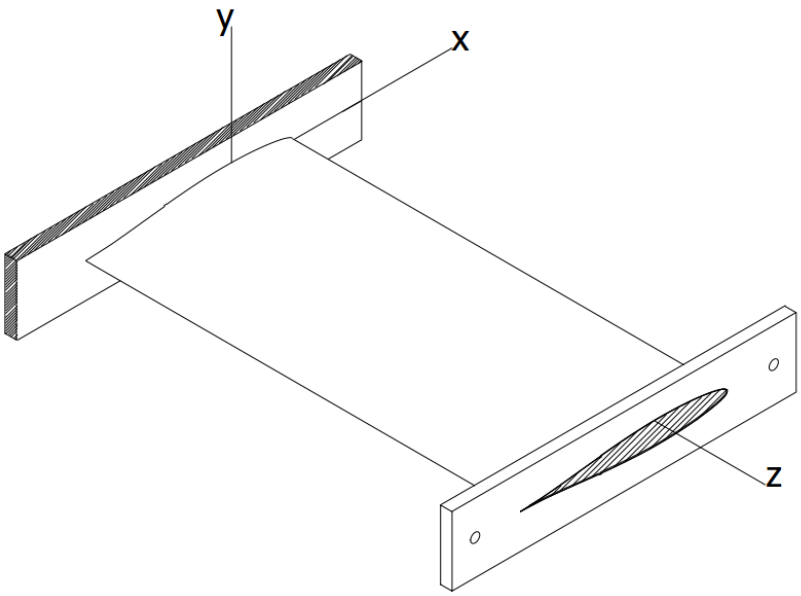

(a) Finite element geometry of the section tail

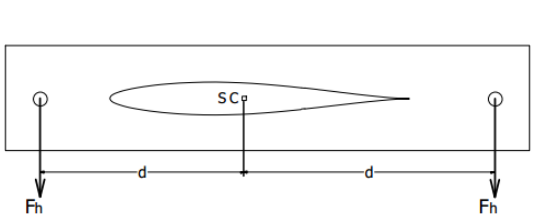

(b) Apply bending momentum to determine bending stiffnesses

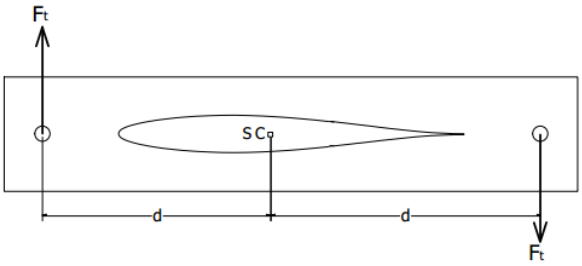

(c) Apply twist momentum to determine torsional stiffnesses

Fig. 3 Approach for determination of bending / torsional stiffnesses

Table 2 Mechanical properties of aluminum isotropic materials

Materials	E (GPa)	ν (GPa)	**ρ** (kg/m^3)
Al	70	0.3	2700

The finite element simulation as shown in Fig. 4, for various thicknesses and different materials have applied and bending/torsional stiffnesses are obtained. Various thicknesses as 0.5, 1, 1.5 and 2 mm have studied, and aluminum isotropic material have discussed. Mechanical properties of aluminum isotropic material are mentioned in Table 2. The E, ν and **ρ** denoted to elastic modulus, Poisson's ratio and density of aluminum metal.

For various thicknesses of aluminum, the bending and torsional stiffnesses, the bending and torsional frequencies and ratio of the uncoupled bending to torsional frequencies have determined and mentioned in Table 3. The results in Table 3 show that although the change of bending frequency is small, but the change of torsional frequency is significant.

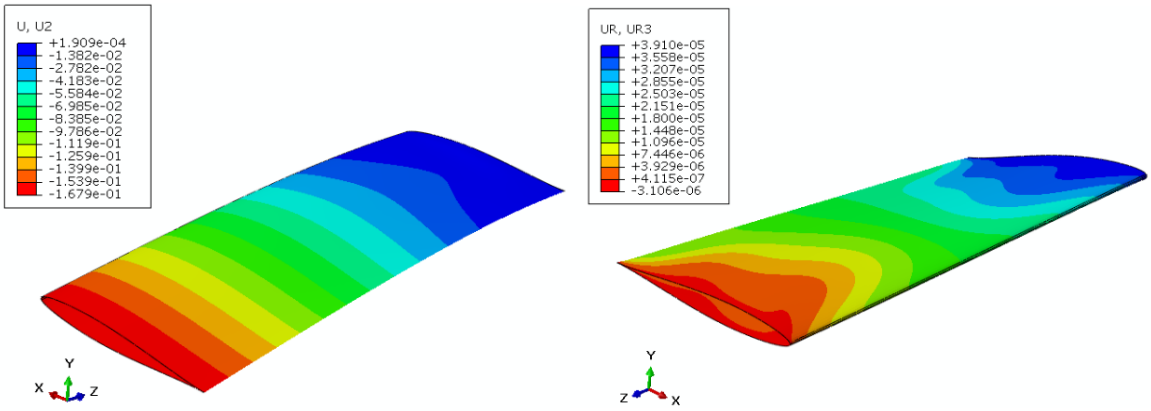

(a) Bending stiffnesses (b) Torsional stiffnesses

Fig. 4 Finite element simulation analysis to obtain

Table 3 Bending and torsional characterization of the thin-airfoil section for various thicknesses of isotropic materials

Thickness: t (mm)	k_h (N/m)	k_θ (N.m/rad)	ω_h(Hz)	ω_θ (Hz)	σ
0.5	20792.3	9698.6	133.7	572.1	0.234
1	40816.3	18797.0	133.4	589.8	0.226
1.5	59701.5	27252.9	132.6	600.2	0.221
2	77821.0	35112.4	131.7	607.8	0.217

3.2 Flutter analysis of tail section

After determining the geometrical and physical parameters of airfoil section, the flutter analysis of isotropic sections is investigated. For this purpose, using the quasi-steady method for two degrees of freedom of the airfoil, the flutter speeds results in incompressible flow for aluminum materials based on governing equations are calculated and plotted.

3.3 Flutter of aluminum skin

In this section to study the flutter speed, we consider a specific section of an aluminum V-tail section. Substituting the aluminum parameters to the governing equations, the behavior of the complex roots as functions of V to find of divergent and flutter speed is investigated. Plots of the real and imaginary parts of the roots versus V are shown in Figs. 5 and 6, respectively. The real part of modal frequencies is shown the modal damping and divergence speed as plotted in Fig. 5. This figure shows that when the skin thickness increases, divergence speed will increase.

By the imaginary part of the modal frequency solution, the main graph of the flutter speed is obtained and plotted in Fig. 6. The Fig. 6, demonstrated both flutter and divergence speeds. Flutter point is located in torsional and bending (plunging) modal frequency coalesce. The results of divergences and flutter speed for the aluminum shell with different thicknesses in km/h are derived and mentioned in Table 4. These results show that with increasing the thickness, the divergences speed and flutter speed have increased.

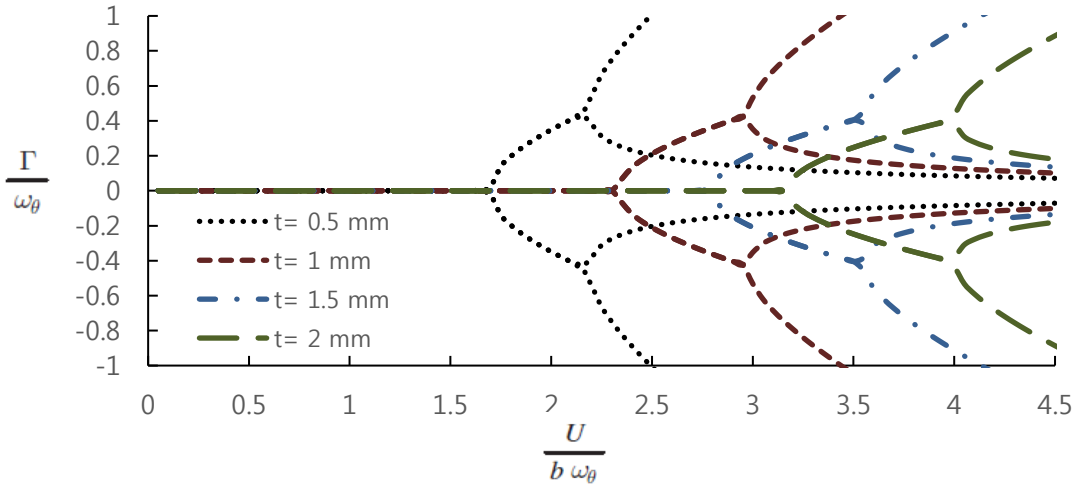

Fig. 5 The imaginary part of modal solution, indicate the modal frequency versus V for aluminum shell

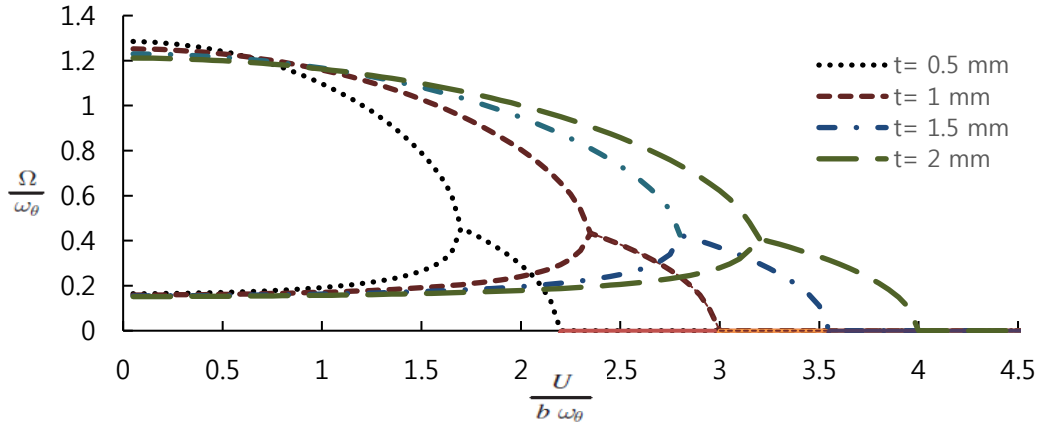

Fig. 6 The imaginary part of modal solution, indicate the modal frequency versus V for aluminum shell

Table 4 Flutter and divergence speeds for aluminum section

Thickness: t (mm)	0.5	1	1.5	2
V- Flutter (km/h)	928	1310	1603	1853
V- Divergence(km/h)	1260	1841	2234	2555

3.4 Discussion and comparisons

The results of Table 4, for various thicknesses of isotropic materials, is remarkable. The flutter speed versus the shell thickness for different types of sections is calculated and shown in Fig. 7.

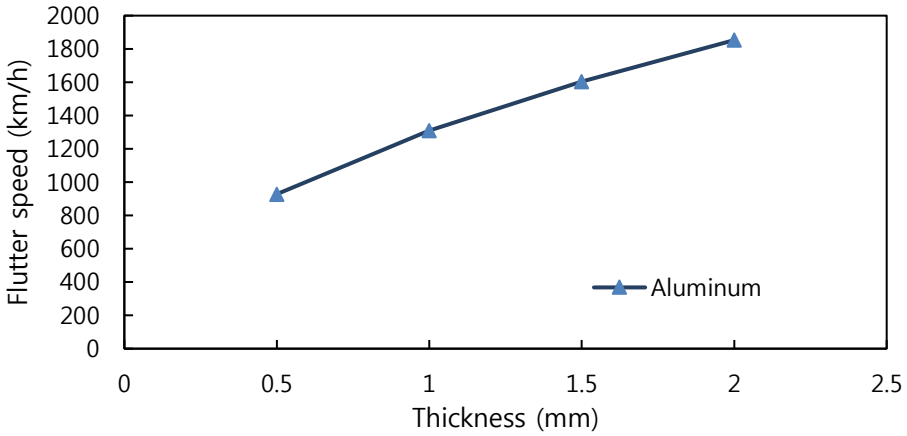

Fig. 7 Comparison the flutter speed versus the shell thickness sections

Table 5 Discrepancy of flutter speeds for an aluminum section between results obtained from this research and primary equation (Eq. (11)) (Kumar *et al*. 2020)

Skin thickness (mm)	0.5	1	1.5	2
Flutter speed (km/h) (this study)	928	1310	1603	1853
Flutter speed (km/h) (NACA RM L7G02)	858	1210	1471	1686
Discrepancy (%)	7.5%	7.6%	8.2%	9.0%

The results show that with increasing the thickness of shell section the flutter speed increased and from 928 km/h for 0.5 mm shell thickness raised to 1853 km/h for 2 mm shell thickness.

3.5 Validation

In this section, the analytical- numerical coupled model of the flutter in tail section based on the bending– torsional coupling is validated with an approximate model (Budiansky *et al*. 1947). As this presented equation based on torsional stiffness, therefore it is conservative. It is rewritten according to this research symbols as follows:

$$V_f = b.\omega_\theta \sqrt{\frac{r_f^2}{k_f}\frac{\frac{1}{2}}{\frac{1}{2}+e}} \tag{11}$$

where k_f is the ratio of the mass of air (for diameter cylinder equal to the chord of the wing) to the mass of the wing, that both of them are taken for the length equals the span of the wing. Also, r_f is the ratio of mass radius of gyration referred to shear center to the half- chord of the airfoil section.

The calculated flutter speed obtained in this research can be compared to the results obtained from Eq. (11). These results for an aluminum section for various thicknesses based on primary Eq. (11) and results of the coupling-torsional coupling in this research are presented in Table 5. These

results show that this approach has good agreements with other methods, and percent discrepancy between these two methods are less than 10%. As the primary Eq. (11) based on torsional stiffnesses and disregarding the bending stiffnesses, it seems that this discrepancy between results is not out of reality and is acceptable for validating this research results.

4. Conclusions

Using the quasi-steady method for two degrees of freedom of airfoil section for the V-tail of aircraft, the divergence and flutter speeds in the incompressible flow were calculated and discussed. The method is based on the bending-torsional coupling of the V-tail section of the aircraft. The geometry and physical parameters as the aerodynamic center, shear center, mass center, bending, and torsional frequencies are determined using the simulation method in ANSYS finite element commercial software. Furthermore, for various thicknesses, the divergence and flutter speed are obtained and discussed. Also, the results compared with the primary equation in the literature. Based on the results of this work, the following conclusions were obtained:

• For an isotropic material, with increasing the thickness the bending and torsional stiffnesses are increased, but only the change of torsional frequency is significant.

• Using finite element analysis the geometry parameters and bending/torsional momentums can be obtained.

• With increasing the shell thickness the flutter and divergence speeds were increased.

• In the bending–torsional coupling method of V-tail section the torsional stiffnesses and frequencies are more effective than bending stiffnesses and frequencies.

The primary equations for estimating flutter speed based on torsional stiffness predicted the values of flutter speed about 10% lower than with determined in this research.

References

Aleksandrowicz, R. and Lucjanek, W. (1958), "Sailplane stiffness measurements", *OSTIV Publications*, **5**.

Borri, C. and Costa, C. (2004), "A parametric study of indicial function models in bridge deck aeroelasticity", *Wind Struct.*, **7**(6), 405-420. http://dx.doi.org/10.12989/was.2004.7.6.405.

Budiansky, B., Kotanchik, J.N. and Chiarito, P.T. (1947), *A Torsional Stiffness Criterion for Preventing Flutter of Wings of Supersonic Missiles*, National Advisory Committee for Aeronautics Langley Field Va Langley Aeronautical Laboratory.

Cai, J., Zhang, Q., Jiang, Y., Xu, Y., Feng, J. and Deng, X. (2017), "Nonlinear stability analysis of a radially retractable hybrid grid shell in the closed position", *Steel Compos. Struct.*, **24**(3), 287-296. https://doi.org/10.12989/scs.2017.24.3.287.

Diana, G., Resta, F., Zasso, A., Belloli, M. and Rocchi, D. (2004), "Effects of the yaw angle on the aerodynamic behaviour of the Messina multi-box girder deck section", *Wind Struct.*, **7**(1), 41-54. http://dx.doi.org/10.12989/was.2004.7.1.041.

Dillinger, J.K.S., Klimmek, T., Abdalla, M.M. and Gürdal, Z. (2013), "Stiffness optimization of composite wings with aeroelastic constraints", *J. Aircraft*, **50**(4), 1159-1168. https://doi.org/10.2514/1.C032084.

Ding, Q., Chen, A. and Xiang, H. (2002), "A state space method for coupled flutter analysis of long-span bridges", *Struct. Eng. Mech.*, **14**(4), 491-504. http://dx.doi.org/10.12989/sem.2002.14.4.491.

Eltaher, M.A. and Mohamed, S.A. (2020), "Buckling and stability analysis of sandwich beams subjected to varying axial loads", *Steel Compos. Struct.*, **34**(2), 241-260. https://doi.org/10.12989/scs.2020.34.2.241.

Evans, S.P., Bradney, D.R. and Clausen, P.D. (2018), "Development and experimental verification of a 5kW

small wind turbine aeroelastic model", *J. Wind Eng. Ind. Aerod.*, **181**, 104-111. https://doi.org/10.1016/j.jweia.2018.08.011.

Ghasemi, A.R., Jahanshir, A. and Tarighat, M.H. (2014), "Numerical and analytical study of aeroelastic characteristics of wind turbine composite blades", *Wind Struct.*, **18**(2), 103-116. http://dx.doi.org/10.12989/was.2014.18.2.103.

Ghasemi, A.R. and Mohandes, M. (2016), "Composite blades of wind turbine: Design, stress analysis, aeroelasticity, and fatigue", *Wind Turb. Des. Control Appl.*, 1-26. http://dx.doi.org/10.5772/63446.

Grinderslev, C., Lubek, M. and Zhang, Z. (2018), "Nonlinear fluid-structure interaction of bridge deck: CFD analysis and semi-analytical modeling", *Wind Struct.*, **27**(6), 381-397. http://dx.doi.org/10.12989/was.2018.27.6.381.

Hodges, D.H. and Pierce, G.A. (2011), *Introduction to Structural Dynamics and Aeroelasticity (Vol. 15)*. Cambridge university press.

Kumar, S., Onkar, A.K. and Manjuprasad, M. (2020), "Stochastic modeling and reliability analysis of wing flutter. journal of aerospace engineering", **33**(5), 04020044. https://doi.org/10.1061/(ASCE)AS.1943-5525.0001153.

Lair, J., Hui, D., Sofiyev, A.H., Gribniak, V. and Turan, F. (2019), "On the parametric instability of multilayered conical shells using the FOSDT", *Steel Compos. Struct.*, **31**(3), 277-290. https://doi.org/10.12989/scs.2019.31.3.277.

Li, Z., Wen, B., Dong, X., Peng, Z., Qu, Y. and Zhang, W. (2020), "Aerodynamic and aeroelastic characteristics of flexible wind turbine blades under periodic unsteady inflows", *J. Wind Eng. Ind. Aerod.*, **197**, 104057. https://doi.org/10.1016/j.jweia.2019.104057.

Mahmoud, S.R. and Tounsi, A. (2019), "On the stability of isotropic and composite thick plates", *Steel Compos. Struct.*, **33**(4), 551-568. https://doi.org/10.12989/scs.2019.33.4.551.

Marzani, A. and Viola, E. (2003), "Effect of boundary conditions on the stability of beams under conservative and non-conservative forces", *Struct. Eng. Mech.*, **16**(2), 195-217. http://dx.doi.org/10.12989/sem.2003.16.2.195.

Mastroddi, F., Tozzi, M. and Capannolo, V. (2011), "On the use of geometry design variables in the MDO analysis of wing structures with aeroelastic constraints on stability and response", *Aerosp. Sci. Technol.*, **15**(3), 196-206. https://doi.org/10.1016/j.ast.2010.11.003.

Mousavi, S.B. and Yazdi, A.A. (2019), "Aeroelastic behavior of nano-composite beam-plates with double delaminations", *Steel Compos. Struct.*, **33**(5), 653-661. http://dx.doi.org/10.12989/scs.2019.33.5.653.

Omenzetter, P., Wilde, K. and Fujino, Y. (2000), "Suppression of wind-induced instabilities of a long span bridge by a passive deck–flaps control system: Part I: formulation", *J. Wind Eng. Ind. Aerod.*, **87**(1), 61-79.

Shafei, E. and Shirzad, A. (2017), "Ant colony optimization for dynamic stability of laminated composite plates", *Steel Compos. Struct.*, **25**(1), 105-116. https://doi.org/10.12989/scs.2017.25.1.105.

Stodieck, O., Cooper, J.E., Weaver, P.M. and Kealy, P. (2017), "Aeroelastic tailoring of a representative wing box using tow-steered composites", *AIAA J.*, **55**(4), 1425-1439. https://doi.org/10.2514/1.J055364.

Taheri-Behrooz, F. and Omidi, M. (2018), "Buckling of axially compressed composite cylinders with geometric imperfections", *Steel Compos. Struct.*, **29**(4), 557-567. https://doi.org/10.12989/scs.2018.29.4.557.

Wang, Q. (2003), "On complex flutter and buckling analysis of a beam structure subjected to static follower force", *Struct Eng. Mech.*, **16**(5), 533-556. http://dx.doi.org/10.12989/sem.2003.16.5.533.